methylidene-GMP, 16628-88-9; phosphoenolpyruvate carboxykinase, 9013-08-5.

References

Blättler, W. A., & Knowles, J. R. (1979a) *J. Am. Chem. Soc. 101*, 510–511.
Blättler, W. A., & Knowles, J. R. (1979b) *Biochemistry 18*, 3927–3933.
Brown, D. M., Fried, M., & Todd, A. R. (1953) *Chem. Ind. (London)*, 352–353.
Chang, H. C., Maruyama, H., Miller, R. S., & Lane, M. D. (1966) *J. Biol. Chem. 241*, 2421–2430.
Duffy, T. H., Markovitz, P. J., Chuang, D. T., Utter, M. F., & Nowak, T. (1981) *Proc. Natl. Acad. Sci. U.S.A. 78*, 6680–6683.
Frey, P. A. (1982a) *Tetrahedron 38*, 1541–1567.
Frey, P. A. (1982b) in *New Comprehensive Biochemistry* (Neuberger, A., & Van Deenen, L. L. M., Eds.) Vol. 3, pp 201–248, Elsevier Biomedical, Amsterdam.
Miller, R. S., & Lane, M. D. (1968) *J. Biol. Chem. 243*, 6041–6049.
Noce, P., & Utter, M. F. (1975) *J. Biol. Chem. 250*, 9091–9105.
Orr, G. A., Simon, J., Jones, S. R., Chin, G., & Knowles, J. R. (1978) *Proc. Natl. Acad. Sci. U.S.A. 75*, 2230–2233.
Richard, J. P., & Frey, P. A. (1978) *J. Am. Chem. Soc. 100*, 7757–7758.
Richard, J. P., & Frey, P. A. (1982) *J. Am. Chem. Soc. 104*, 3476–3481.
Richard, J. P., Ho, H.-T., & Frey, P. A. (1978) *J. Am. Chem. Soc. 100*, 7756–7757.
Sheu, K. F. R., Richard, J. P., & Frey, P. A. (1979) *Biochemistry 18*, 5548–5556.
Webb, M. R. (1982) *Methods Enzymol. 87*, 301–316.
Whitfield, P. R., & Markham, R. (1953) *Nature (London) 171*, 1151–1152.

Some Aspects of the Mechanism of Complexation of Red Kidney Bean α-Amylase Inhibitor and α-Amylase†

Edward R. Wilcox‡ and John R. Whitaker*

ABSTRACT: Bovine pancreatic α-amylase binds 1 mol of acarbose (a carbohydrate α-amylase inhibitor) per mol at the active site and also binds acarbose nonspecifically. The red kidney bean α-amylase inhibitor–bovine pancreatic α-amylase complex retained nonspecific binding for acarbose only. Binding of *p*-nitrophenyl α-D-maltoside to the final complex of red kidney bean α-amylase inhibitor and bovine pancreatic α-amylase has a βK_s (K_s') value that is 3.4-fold greater than the K_s (16 mM) of α-amylase for *p*-nitrophenyl α-D-maltoside alone. The initial complex of α-amylase and inhibitor apparently hydrolyzes this substrate as rapidly as α-amylase alone. The complex retains affinity for substrates and competitive inhibitors, which, when present in high concentrations, cause dissociation of the complex. Maltose (0.5 M), a competitive inhibitor of α-amylase, caused dissociation of the red kidney bean α-amylase inhibitor–α-amylase complex. Interaction between red kidney bean (*Phaseolus vulgaris*) α-amylase inhibitor and porcine pancreatic α-amylase proceeds through two steps. The first step has a K_{eq} of 3.1×10^{-5} M. The second step (unimolecular; first order) has a forward rate constant of 3.05 min^{-1} at pH 6.9 and 30 °C. α-Amylase inhibitor combines with α-amylase, in the presence of *p*-nitrophenyl α-D-maltoside, noncompetitively. On the basis of the data presented, it is likely that α-amylase is inactivated by the α-amylase inhibitor through a conformational change. A kinetic model, in the presence and absence of substrate, is described for noncompetitive, slow, tight-binding inhibitors that proceed through two steps.

The proteinaceous α-amylase inhibitor of red kidney bean (*Phaseolus vulgaris*) has been purified to homogeneity (E. R. Wilcox and J. R. Whitaker, unpublished results). This inhibitor is slow in inactivating α-amylase, but it is tight binding. Depending on pH and concentrations of reactants, the red kidney bean α-amylase inhibitor can take several hours to inactivate porcine pancreatic α-amylase (Powers & Whitaker, 1977b). The slowness of the inactivation could be caused by a requirement for a conformational change in either the inhibitor or α-amylase or both (Powers & Whitaker, 1977b). The time required to inhibit α-amylase by other amylase inhibitors appears to be dependent on the source of α-amylase and α-amylase inhibitor as well as on the concentrations of inhibitor and enzyme and the pH. O'Connor & McGeeney (1981a,b) found a 60 000-dalton wheat α-amylase inhibitor that inhibited human salivary α-amylase much quicker than human pancreatic α-amylase. After a 0.5-h preincubation step to permit complexation, the ratio of salivary to pancreatic α-amylase inhibition was 140.

Powers & Whitaker (1977b) showed that the porcine pancreatic α-amylase–red kidney bean α-amylase inhibitor complex, when treated with maltose, has a concentration-dependent absorption change, suggesting that the complex can still bind the competitive inhibitor, maltose. The K_i calculated for maltose binding to the complex was 13 mM. Elodi et al. (1972) reported that maltose causes a concentration-dependent absorption change at 291 nm when it binds to porcine pancreatic α-amylase. The K_i (13 mM) of maltose, on the basis of this absorbance change, is in agreement with the K_i of 25 mM for maltose binding to α-amylase as determined from activity assays (inhibitor). This is indicative that the active site of α-amylase is still partially or fully available when the red kidney bean inhibitor is bound to the enzyme.

Proteinaceous α-amylase inhibitors bind tightly to mammalian α-amylases. Red kidney bean inhibitor has a K_i of 3

† From the Department of Food Science and Technology, University of California, Davis, Davis, California 95616. *Received August 1, 1983.*
‡ Present address: Department of Neurosciences, School of Medicine, University of California, San Diego, La Jolla, CA 92093.

0006-2960/84/0423-1783$01.50/0

$\times 10^{-11}$ M (Powers & Whitaker, 1977b). Because the inhibitor is both slow and tight binding, special considerations have to be made in regard to the kinetics of the reactions (Green, 1953; Bieth, 1974; Cha, 1977, 1980; Williams & Morrison, 1979; Williams et al., 1979). Michaelis–Menten kinetics are not applicable; non-steady-state kinetics must be used. To date, no published study has elucidated the type of inhibition exhibited by the proteinaceous α-amylase inhibitors. The purpose of this research is to better understand how porcine pancreatic α-amylase is inhibited by red kidney bean inhibitor.

Materials and Methods

Materials. Porcine pancreatic α-amylase (type I-A, 2 times crystallized, lots 60F-8105 and 87C-83251), bovine serum albumin (fraction V, lot 111C-2760), bovine pancreatin (lot 558-0220), and glycogen (type II) were obtained from Sigma Chemical Co. Red kidney bean α-amylase inhibitor, purified as described by E. R. Wilcox and J. R. Whitaker (unpublished results), was homogeneous by disc gel electrophoresis. Acarbose (Truscheit et al., 1981; structure I) was a gift from

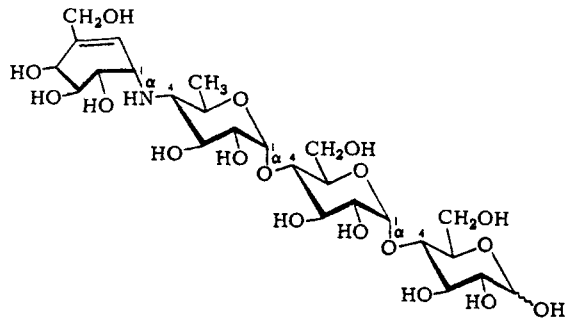

I, *O*-4,6-dideoxy-4-[[4,5,6-trihydroxy-3-(hydroxymethyl)-2-cyclohexen-1-yl]amino]-α-D-glucopyranosyl-(1→4)-*O*-α-D-glucopyranosyl-(1→4)-D-glucose

Dr. E. Truscheit and Prof. Dr. W. Frommer of Bayer AG, West Germany. Maltose and *p*-nitrophenyl α-D-maltoside (lots 040102 and 110044) were obtained from Calbiochem Corp. Sodium [^{3}H]borohydride (sp act. 350 mCi/mmol, lot 997604) was from ICN. Maltrin M-100 (lot C-2463) was a gift from Grain Processing Corp., Musatine, IA 52761. Maltrin M-100 is starch solubilized by brief acid–brief enzyme treatment (Morehouse et al., 1972), with limited increase in low molecular compounds.

All other chemicals used were reagent grade. All water used was double-deionized water.

Protein Determinations. Molarity of α-amylase solutions was determined from the absorbance at 280 nm, on the basis of a molecular weight of 52 000 and $A^{1\%}_{1cm} = 24.0$ (Elodi et al., 1972). Molar inhibitor concentrations were determined from the weight of lyophilized protein, on a Cahn Electrobalance, and a molecular weight of 49 000 (Powers & Whitaker, 1977a). Bovine serum albumin was used as a standard in the Lowry method (Lowry et al., 1951).

Assays for α-Amylase and Inhibitor Activities. Activity assays for α-amylase and α-amylase inhibitor were determined by a modification of the Bernfeld method (1955) as described previously (E. R. Wilcox and J. R. Whitaker, unpublished results).

Purification of Bovine Pancreatic α-Amylase. For the kinetic studies, isozyme II (Marchis-Mouren & Pasero, 1967) of bovine pancreatic α-amylase was used. Glycogen precipitation of α-amylase was performed as described by Schramm & Loyter (1966). To remove limit dextrins, α-amylase was passed through a DEAE-cellulose column equilibrated with 5 mM phosphate buffer, pH 8.0 (Marchis-Mouren & Pasero, 1967). α-Amylase isozyme II is the second peak with α-amylase activity eluted from this column (sp act. 1000 units/mg). Combined fractions of this second peak were pooled, dialyzed, lyophilized, and rechromatographed on DEAE-cellulose under the same conditions just described. The α-amylase peak had a constant specific activity across the peak (1400 units/mg) and was homogeneous by disc gel electrophoresis (40 μg of protein used). One unit is the amount of α-amylase that catalyzes the formation of 1 mg equiv of maltose hydrate in 3 min at 30 °C in sodium phosphate buffer, pH 6.9.

Starch-Binding Experiments. Unswollen starch granules were suspended several times in 0.05 M phosphate buffer, pH 6.9, containing 0.25 M NaCl and 1 mM $CaCl_2$ (standard buffer). The granules were sized in standard buffer, and columns were made from Pasteur pipets with glass wool at the neck. These columns were washed with several milliliters of buffer before a solution containing 0.2 mg of porcine pancreatic α-amylase alone, 0.1 mg of inhibitor alone, or a mixture of 0.1 mg of inhibitor and 0.2 mg of α-amylase was layered on top. Fractions (1.6 mL) were collected, and the absorbance was monitored at 230 nm. Maltose (0.5 M) in the standard buffer was used to elute α-amylase or inhibitor–α-amylase complex from these columns.

Dissociation of Enzyme–Inhibitor Complex with Maltose. Pure α-amylase inhibitor (250 mg) was covalently bound to 50 mL of activated Sepharose 2B as described by Cuatrecasas & Anfinsen (1971). The Sepharose was activated with 2.5 gm of CNBr. After preparation of the affinity gel, a column was poured (1.5 × 25 cm) and was washed with 500 mL of 0.1 M sodium borate buffer, pH 9, containing 1 M NaCl. This was followed with 500 mL of 0.1 M sodium acetate buffer, pH 4.5, containing 1 M NaCl. The column was equilibrated with 0.05 M phosphate buffer, pH 6.9, containing 0.25 M NaCl and 1 mM $CaCl_2$ (standard buffer) before the addition of a solution, in the same buffer, of 770 units of porcine pancreatic α-amylase. Elution was done with 0.5 M maltose in standard buffer, followed by 0.1 M glycine buffer, pH 3.0, containing 0.05 M NaCl and 1 mM $CaCl_2$.

Binding of [^{3}H]Acarbose to α-Amylase and α-Amylase–Inhibitor Complex. A total of 5 mg of [^{3}H]$NaBH_4$ (50 mCi/mmol) was added to 5 mg of acarbose dissolved in 1 mL of water and the solution incubated at 37 °C for 1.5 h, thereby reducing the terminal D-glucose of acarbose (structure I) to D-sorbitol. The excess $NaBH_4$ was destroyed by addition of a few drops of acetic acid (until no more gas was evolved; done in a fume hood). This solution was lyophilized, and 1.5 mL of methanol was added to remove borate by lyophilization (Warner & O'Brien, 1982). Addition of methanol and lyophilization were repeated 3 times. The ^{3}H-reduced acarbose was made to 1.55 mM by the addition of 5 mL of standard buffer. For kinetic determinations, nonradioactive $NaBH_4$-reduced acarbose was prepared by the above method.

Solutions of bovine α-amylase (1×10^{-5} M) and bovine α-amylase–red kidney bean α-amylase inhibitor complex (1×10^{-4} M inhibitor with 1×10^{-5} M α-amylase) were each dialyzed against two changes of standard buffer. The molarity of α-amylase was then checked by absorbance at 280 nm. Aliquots of α-amylase or α-amylase–inhibitor complex (1.0 mL) were placed into washed dialysis tubing along with 9 mL of ^{3}H-reduced acarbose in standard buffer. The concentration of ^{3}H-reduced acarbose was varied from 2.5×10^{-6} to 7.5×10^{-5} M. The solutions were allowed to reach equilibrium for 48 h at 4 °C. Then, two aliquots (0.2 mL each) were removed

from inside and outside the dialysis tubing into 10 mL of Aquasol and counted by standard scintillation counting techniques.

Assays for α-Glucosidase. Bovine α-amylase (isoenzyme II), purified in this laboratory, was tested for contamination by other α-glucosidases. α-Amylase (2.5×10^{-7} M, final concentration) was incubated with 20 mM maltose at 30 °C in standard buffer, pH 6.9, for up to 40 min before the addition of 1 mL of dinitrosalicylic acid (DNS) reagent (Bernfeld, 1955). All samples were then diluted 7-fold into DNS reagent before a boiling for 5 min. This step is necessary because maltose was not reduced prior to its use as a substrate. Samples were then diluted by the addition of 10 mL of H_2O and read against water. Blanks contained only maltose.

Kinetic Analyses. The data obtained from kinetic studies of the rate of complexation of α-amylase inhibitor with α-amylase in the presence of *p*-nitrophenyl α-D-maltoside as substrate were analyzed by three models. Cha (1976, 1980) has described the kinetics of slow, tight-binding inhibitors. He assumed that the reaction between enzyme and substrate is at equilibrium, that the amount of substrate used during the data collection from a progress curve is insignificant compared to the total substrate present, and that the reaction between enzyme and inhibitor is established slowly (model A). When

model A

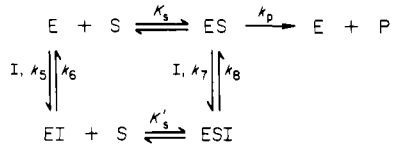

the inhibitor concentration is at a level where significant depletion by enzyme occurs, eq 1 represents the formation of

$$P = v_s t + \frac{(1-\nu)(v_0 - v_s)}{\lambda \nu} \ln\left[\frac{1 - \nu \exp(-\lambda t)}{(1-\nu)}\right] \quad (1)$$

product, P, with respect to time t, v_0 is the velocity of enzyme in the absence of inhibitor, v_s is the velocity once equilibrium between enzyme and inhibitor is reached, and λ is a combination of rate constants that will vary with inhibitor and substrate concentration according to eq 2. ν is the depletion factor for inhibitor concentration. This constant is set in terms of the other three rate constants by eq 5

$$\lambda = \alpha + \beta[\mathrm{I}] \quad (2)$$

where

$$\alpha = \frac{k_6 + k_8[\mathrm{S}]/K_s'}{1 + [\mathrm{S}]/K_s'} \quad (3)$$

and

$$\beta = \frac{k_5 + k_7[\mathrm{S}]/K_s}{1 + [\mathrm{S}]/K_s} \quad (4)$$

$$\nu = ([\mathrm{E}]_0/[\mathrm{I}]_0)(1 - v_s/v_0) \quad (5)$$

The second model (model B) was that of Williams et al.

model B

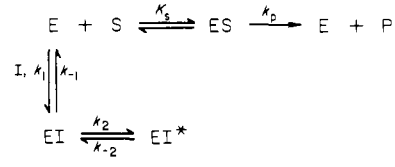

(1979). Williams et al. (1979) found it necessary to include a second step (EI ⇌ EI*) involving enzyme and inhibitor (model B) to explain the kinetics of a competitive inhibitor. They assumed that [ES], [E], and [EI] were at steady state. In this model, the amount of substrate used in product formation is assumed to be insignificant, and k_p is assumed to be much less than k_{-1} (for $K_m \simeq K_s$). This model is described kinetically by eq 6–9

$$0 = [\mathrm{EI}]^2 - [\mathrm{EI}]([\mathrm{E}'] + [\mathrm{I}'] + K_i') + [\mathrm{E}'][\mathrm{I}'] \quad (6)$$

$$[\mathrm{ES}] = ([\mathrm{E}'] - [\mathrm{EI}])/(1 + K_m/[\mathrm{S}]) \quad (7)$$

$$\frac{d[\mathrm{EI}^*]}{dt} = k_2[\mathrm{EI}] - k_{-2}[\mathrm{EI}^*] \quad (8)$$

$$\frac{d[\mathrm{P}]}{dt} = k_p[\mathrm{ES}] \quad (9)$$

where $[\mathrm{E}'] = [\mathrm{E_T}] - [\mathrm{EI}^*]$, $[\mathrm{I}'] = [\mathrm{I_T}] - [\mathrm{EI}^*]$, $K_i' = K_{eq}(1 + [\mathrm{S}]/K_m)$, $K_{eq} = k_{-1}/k_1$, and $K_m = K_s$.

Numerical integration can be performed on eq 8 and 9 when the initial conditions are known. In our case, the initial conditions were [P] = 0.0 and [EI*] = 0.0 when t = 0.0. The concentrations of EI and ES were calculated from eq 6 and 7. CRICF (Chandler et al., 1972) was used to perform the numerical integrations and least-squares fit of the data to progress [P] vs. t curves.

A still more complex kinetic model (model C) was required

model C

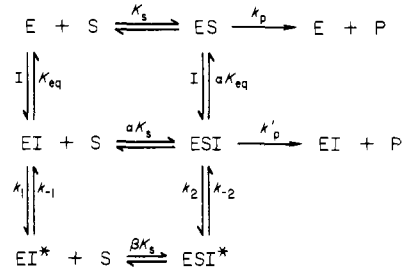

to fit progress curves to rate equations when substrate concentrations were greater than K_m. The model assumes that [E], [ES], [EI], and [ESI] are at steady state. The model also assumes that the interconversion of EI* and ESI* is at steady state and that the amount of substrate converted to product during the measurements is insignificant in comparison to total substrate present and also assumes $K_m \simeq K_s$. Equations 10–20 describe this model in terms of [ES]

$$[\mathrm{I}] = [\mathrm{I}]_0 - [\mathrm{E}]_0 + [\mathrm{ES}](1 + K_s/[\mathrm{S}]) \quad (10)$$

$$[\mathrm{ESI}] = [\mathrm{ES}][\mathrm{I}]/(\alpha K_i) \quad (11)$$

$$[\mathrm{EI}] = [\mathrm{I}][\mathrm{ES}]K_s/(K_i[\mathrm{S}]) \quad (12)$$

$$[\mathrm{EI}^*] = \frac{[\mathrm{E}]_0 - [\mathrm{ES}]\left(1 + \frac{K_s}{[\mathrm{S}]} + \frac{[\mathrm{I}]}{\alpha K_i} + \frac{[\mathrm{I}]K_s}{K_i[\mathrm{S}]}\right)}{1 + [\mathrm{S}]/(\beta K_s)} \quad (13)$$

$$[\mathrm{ESI}^*] = \frac{[\mathrm{S}]}{\beta K_s}[\mathrm{EI}^*] \quad (14)$$

$$A = ([\mathrm{S}] + K_s)([\mathrm{I}]_0 - [\mathrm{E}]_0) + \alpha K_i(K_s + [\mathrm{S}]) \quad (15)$$

$$\frac{d[\mathrm{ES}]}{dt} = \alpha K_i[\mathrm{S}]\left[\frac{k_{-1}[\mathrm{EI}^*] + k_{-2}[\mathrm{ESI}^*] - k_1[\mathrm{EI}] - k_2[\mathrm{ESI}]}{\mathrm{A} + 2[\mathrm{ES}](\alpha K_s + [\mathrm{S}])(1 + K_s/[\mathrm{S}])}\right] \quad (16)$$

$$\frac{d[\mathrm{P}]}{dt} = k_p[\mathrm{ES}] + k_p'[\mathrm{ESI}] \quad (17)$$

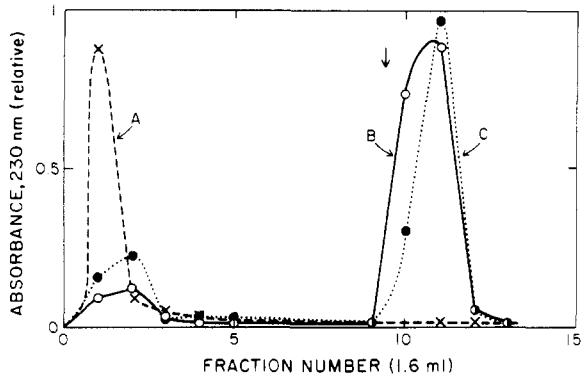

FIGURE 1: Chromatography of inhibitor, α-amylase, and inhibitor–α-amylase complex on starch columns: (A) (×) α-amylase inhibitor alone (0.1 mg); (B) (○) α-amylase alone (0.2 mg); (C) (●) α-amylase inhibitor (0.1 mg) and α-amylase (0.2 mg) preincubated for 6 min or 6 h before application to the column. (↓) Point at which 0.5 M maltose was added as eluant.

At t = 0.0, [EI*] and [ESI*] are assumed to be zero; the concentration of ES can be determined from eq 18–20 where [P] is assumed to be zero. Let

$$AA = ([S] + \alpha K_s)(1 + K_s/[S]) \quad (18)$$

$$BB = ([E]_0 - [I]_0)([S] + \alpha K_s) + \alpha K_i([S] + K_s) \quad (19)$$

then

$$0 = [ES]^2(AA) + [ES](BB) - [E]_0\alpha K_i[S] \quad (20)$$

The above equations were integrated with CRICF (Chandler et al., 1972) and fit to 10 progress curves ([P] vs. t). Derivation of eq 10–20 may be had upon request (see paragraph at end of paper regarding supplementary material).

Results

Starch-Binding Experiments. α-Amylase binds to starch and is eluted from starch by the addition of 0.5 M maltose (Figure 1). α-Amylase inhibitor did not bind to starch columns, but the complex of α-amylase and inhibitor did. The small peak (Figure 1B,C), which came off in the absence of maltose, had no inhibitor or α-amylase activity.

Dissociation of Enzyme–Inhibitor Complex with Maltose. Buonocore et al. (1975) reported that high concentrations of maltose eluted α-amylase previously adsorbed to an affinity column of wheat α-amylase inhibitor. The reversible binding of red kidney bean α-amylase inhibitor to porcine pancreatic α-amylase was tested in a similar manner (Figure 2). α-Amylase was eluted from the column with 0.5 M maltose. The rate of release of α-amylase from the column was slow, as can be seen by the tailing of α-amylase activity from the column. Addition of 0.1 M glycine buffer, pH 3.0, containing 0.05 M NaCl and 1 mM $CaCl_2$ did not elute additional α-amylase. The enzyme–inhibitor complex is known to be rapidly dissociated at pH 3 (Pick & Wober, 1979).

Binding of [^{3}H]Acarbose to α-Amylase and α-Amylase–Inhibitor Complex. A total of 1 mol of ^{3}H-reduced acarbose binds tightly to 1 mol of α-amylase, with several other moles of acarbose binding less tightly (Figure 3). The dissociation constant for the tightly bound acarbose molecule is 9.7×10^{-6} M. This is close to the kinetically determined K_i of 1.8×10^{-5} M for reduced acarbose (done by standard procedures in this laboratory). The tightly bound molecule of acarbose is probably bound at the active site of α-amylase because it binds competitively with substrate.

The complex of α-amylase and red kidney bean α-amylase inhibitor bound several moles of acarbose weakly as did α-amylase alone (nonspecific binding?). The α-amylase inhibitor–α-amylase complex did not bind an acarbose molecule tightly as was found for α-amylase alone (Figure 3).

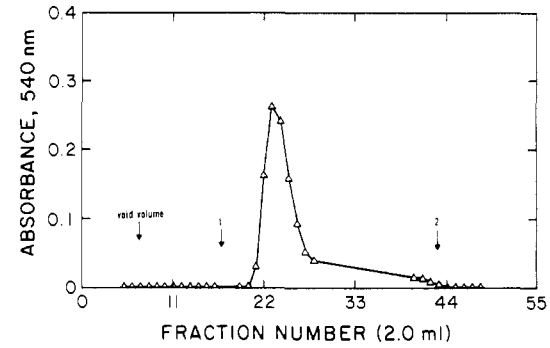

FIGURE 2: Dissociation of enzyme–inhibitor complex with maltose. α-Amylase inhibitor was covalently bound to Sepharose 2B and used as an affinity column. α-Amylase (770 units) was applied in standard buffer, pH 6.9, to the column and eluted with 0.5 M maltose in standard buffer. (↓1) Point at which elution with 0.5 M maltose began. (↓2) Point at which elution with 0.1 M glycine buffer, pH 3.0, containing 0.05 M NaCl and 1 mM $CaCl_2$ began. (△) α-Amylase activity measured by the iodine assay (Banks et al., 1971).

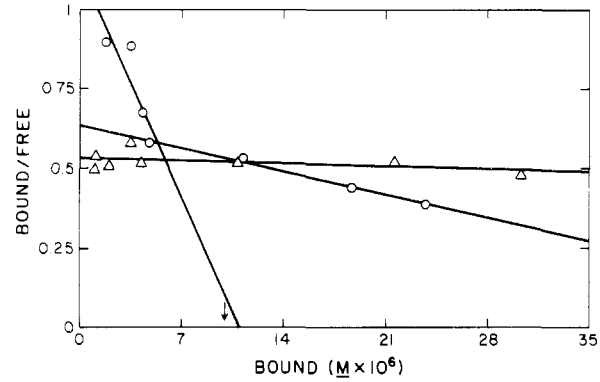

FIGURE 3: Binding of ^{3}H-reduced acarbose to α-amylase and α-amylase–inhibitor complex. (○) α-Amylase (1×10^{-5} M) was incubated in standard buffer, pH 6.9, at 4 °C for 48 h with various concentrations of ^{3}H-reduced acarbose (2.5×10^{-6} to 7.5×10^{-5} M). (△) α-Amylase (1×10^{-5} M) preincubated with red kidney bean inhibitor (1×10^{-4} M) was then incubated with ^{3}H-reduced acarbose. The amount of bound ^{3}H-reduced acarbose was determined by equilibrium dialysis.

These data could be interpreted that the active site of α-amylase is blocked by complexation with the α-amylase inhibitor. Another possible interpretation is that the active site of α-amylase has undergone a conformational change, such that it no longer retains a high specificity for acarbose binding.

Rate of Binding of Inhibitor to α-Amylase. A molar excess of red kidney bean α-amylase inhibitor was added to α-amylase in standard buffer, pH 6.9. Aliquots were removed into maltrin M-100 at different times. The rate of loss of α-amylase activity was first order (Figure 4). When the pseudo-first-order rate constants were plotted as a function of inhibitor concentration (Figure 4 insert), they did not fall on a straight line as is required for a simple one-step reversible process where [I] >> [E].

The model (model D) shown in eq 21 fits these data (Uehara et al., 1980; Gutfreund, 1972).

model D

$$E + I \underset{k_{-1}}{\overset{k_1}{\rightleftharpoons}} EI \underset{k_{-2}}{\overset{k_2}{\rightleftharpoons}} EI^* \quad (21)$$

EI is some complex that is fully active and rapidly reversible during the reactions, EI* is the inactive α-amylase–inhibitor

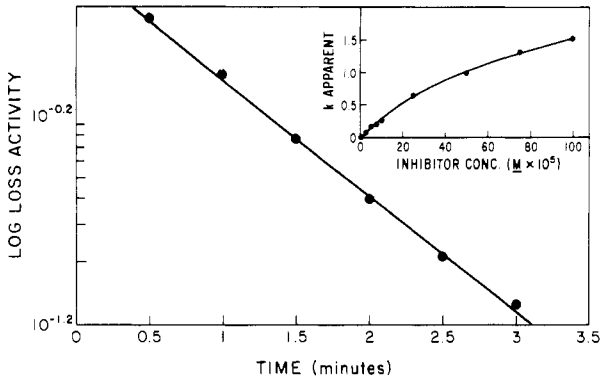

FIGURE 4: Rate of loss of α-amylase activity in the presence of excess inhibitor. Red kidney bean α-amylase inhibitor concentration was 5×10^{-6} M, and the concentration of α-amylase was 10-fold lower (5×10^{-7} M). Aliquots (0.5 mL) of the reaction mixture were withdrawn at different times into 0.5 mL of 5% maltrin M-100. α-Amylase assays were for 3 min at 30 °C in standard buffer, pH 6.9. (Insert) Effect of inhibitor concentration on the observed first-order rate constants. Each k_{app} was determined as shown above. α-Amylase concentration was always 10 times less than the α-amylase inhibitor concentration. The line drawn through the data points is the least-squares fit from eq 22.

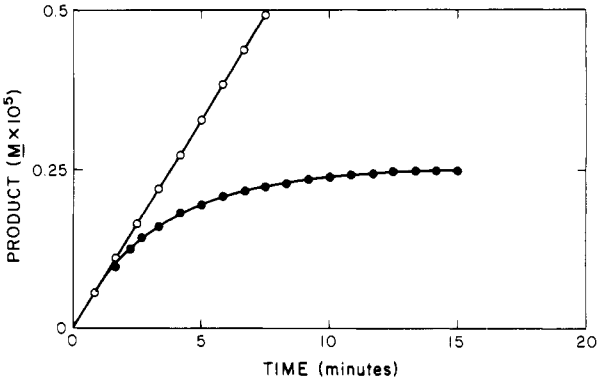

FIGURE 5: Rate of product formation in the presence and absence of inhibitor. (●) The reaction was started by the addition of α-amylase (5×10^{-7} M final concentration) to a mixture of 3×10^{-6} M α-amylase inhibitor and 6 mM p-nitrophenyl α-D-maltoside in standard buffer, pH 6.9, at 30 °C. (○) α-Amylase in absence of α-amylase inhibitor.

Table I: Rate and Equilibrium Constants for Models D and B

rate or equilibrium constants	model D	model B
K_{eq} (M)	$(9.9 \pm 1.2) \times 10^{-6}$	$(1.51 \pm 0.07) \times 10^{-5}$
k_2 (min^{-1})	3.03 ± 0.19	3.05
k_{-2} (min^{-1})	0.0	0.0
absolute percent deviation		5.8

complex and is very slowly reversible ($k_{-2} << k_2$). Equation 22 describes model D (Uehara et al., 1980; Gutfreund, 1972)

$$k_{app} = k_{-2} + \frac{k_2[I]_0}{[I]_0 + K_{eq}} \quad (22)$$

where $K_{eq} = k_1/k_{-1}$.

The curve in the insert of Figure 4 was generated by fitting the experimental data to the above equation. Table I contains the rate constants for model D that best fit the experimental data in Figure 4 (insert).

The overall K_i determined by Powers & Whitaker (1977b) was 3×10^{-11} M. This means that, when eq 23 is used to

$$K_i = \frac{K_{eq}k_{-2}}{k_{-2} + k_2} \quad (23)$$

approximate k_{-2}, the value of k_{-2} is of the order of 10^{-5} min^{-1}. Therefore, the assumption that k_{-2} is zero used in solving eq 22 is valid.

The first step (k_1) in the reaction between α-amylase and inhibitor cannot be measured by steady-state kinetics, because the slow step in the reaction, k_2, is being observed. This also means that, if a second-order rate constant is measured for the reaction ($[I]_0$ is small compared to K_{eq}), the actual measurement is k_2/K_{eq} [see Uehara et al. (1980) and Gutfreund (1972) for a discussion]. The calculated second-order rate constant ($k = k_2/K_{eq}$) consistent with model D would be 5.1×10^3 M^{-1} s^{-1}. Powers & Whitaker (1977b) found a second-order rate constant of 6×10^3 M^{-1} s^{-1} under conditions similar to the above assays. The actual second-order step for the combination of the two macromolecules is probably much more rapid.

Continuous Kinetic Assays Using p-Nitrophenyl α-D-Maltoside. Continuous progress curves ([P] vs. t) generated from the hydrolysis of p-nitrophenyl α-D-maltoside by α-amylase in the presence and absence of inhibitor were digitized and fit to several models. No more than 0.5% of the total substrate was converted to product in any assay. All the assays were run at 30 °C in standard buffer, pH 6.9. Figure 5 is a plot of product formation vs. time in the absence and presence of inhibitor. The decrease in velocity in the presence of the inhibitor vs. the constant velocity in the absence of inhibitor was used to calculate the rate of loss of α-amylase activity due to complex formation and inhibition by the red kidney bean α-amylase inhibitor.

Various concentrations of p-nitrophenyl α-D-maltoside (1–80 mM) and various concentrations of red kidney bean α-amylase inhibitor (1×10^{-7} to 1×10^{-4} M) were incubated together in standard buffer, at pH 6.9, for 10 min at 30 °C. α-Amylase (final concentration of 5×10^{-7} M) was added to start the reaction. The final volume of the mixture was 0.9 mL in a 1-mL cuvette. Activity was monitored at 400 nm for 15–40 min in a Cary spectrophotometer (Model 115C). The extinction coefficient for p-nitrophenol in standard buffer was determined to be 9000 M^{-1} cm^{-1}. Since the extinction coefficient was very sensitive to temperature and pH, it was redetermined for each set of data.

Data were digitized by hand. Ten sets of assays were analyzed at a time with CRICF, a computer program for integrating of rate equations, and least-squares fitting of nonlinear data. The program, prepared by Chandler et al. (1972), was modified for use on a Burroughs 6700 computer.

A Tektronix minicomputer was used to analyze data by the method of Cha (1976, 1980). The Gauss–Newton least-squares software package available on the Textronix was used for this purpose.

When the substrate concentration was less (1–6 mM) than the K_m (16 mM) for the substrate, model B fits the data (Table I and Figure 6). The rate constants agree with those obtained from the pseudo-first-order rate constants (Table I).

Model A also fits these data, but this model is not correct since it does not account for the fact the inhibitor combines with α-amylase by a two-step mechanism (see previous section). A plot of $1/\beta$ (from eq 2) vs. $[S]/K_m$ shows that the inhibitor may be competitive (Figure 7A). This does not necessarily mean that the inhibitor is competitive, as seen in Figure 7B; it only means that k_7 is less than k_5 in model A.

Steady-state velocities for tight-binding inhibitors can be fit with Michaelis–Menten kinetics. However, the interpretation of the results is meaningless. The same problem was found for kinetics describing model A. The constants derived from eq 1 and 2 give a meaningless curve (Figure 7C), when

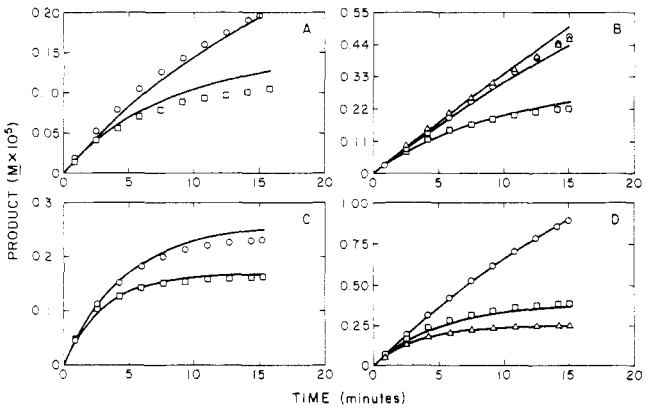

FIGURE 6: Progress curves for the hydrolysis of *p*-nitrophenyl α-D-maltoside by α-amylase in the presence of inhibitor. The curves are fit to model B. Assays were performed at 30 °C in standard buffer, pH 6.9, with an α-amylase concentration of 5×10^{-7} M and substrate concentrations less than K_m. (A) Substrate concentration was 1 mM *p*-nitrophenyl α-D-maltoside. α-Amylase inhibitor concentrations were 4.5×10^{-7} (○) and 9.87×10^{-7} M (□). (B) Substrate concentration was 2 mM *p*-nitrophenyl α-D-maltoside. α-Amylase inhibitor concentrations were 9.5×10^{-8} (△), 2.38×10^{-7} (○), and 9.27×10^{-7} M (□). (C) Substrate concentration was 4 mM *p*-nitrophenyl α-D-maltoside. α-Amylase inhibitor concentrations were 1.98×10^{-6} (○) and 2.95×10^{-6} M (□). (D) Substrate concentration was 6 mM *p*-nitrophenyl α-D-maltoside. α-Amylase inhibitor concentrations were 4.77×10^{-7} (○), 1.98×10^{-6} (□), and 2.97×10^{-6} M (△).

substrate concentrations are greater than K_m.

Ten assays were performed with substrate concentrations greater (20–80 mM) than K_m (16 mM). These data showed an unusual characteristic. Product formation was never fully inhibited by α-amylase inhibitor even at a molar ratio of I to E of 200:1 (Figure 8A). The velocity became constant once equilibrium was reached, and the final velocity (4.6% of that in absence of inhibitor) was dependent on the relative concentration of substrate and inhibitor. When inhibitor was preincubated with enzyme before the addition of substrate, velocity increased with time upon the addition of substrate (Figure 8B,C). Again, the velocity became linear once equilibrium was reached. In either case (Figure 8A,B), the steady-state velocity in the presence of excess inhibitor was 4.6% of the velocity with no inhibitor present (α-amylase inhibitor was 1×10^{-4} M, α-amylase was 5×10^{-7} M, and substrate was 20 mM).

α-Amylase was tested for contamination with other α-glucosidases by incubation of α-amylase with maltose to test for activity; none was found. Inhibitor, when incubated with *p*-nitrophenyl α-D-maltoside, gave no measurable activity in 0.5 h at 30 °C.

In order to fit the data when $[S]_0$ is greater than K_m, model C was required (Figure 9 and Table II). Model B failed to fit the data (Table II), as did model A (Figure 7C).

Because k_1 correlates with K_{eq} to a very high degree (99%), it was assumed to be 3.05 min^{-1} (Table II) and fixed at that value. Rate constants k_{-1} and k_2 were assumed to be zero, since the least-squares fitting of the data tended to that value. The correlation matrix and error analysis of model C, with calculated rate and equilibrium constants, are shown in Table III.

Model C implies that ESI forms product at the same rate as ES. If k_p' is set to zero and a new least-squares solution obtained, the model changes to the poor fitting competitive inhibition model (α goes to infinity and k_{-2} goes to zero). This implies that a considerable fraction of product formed (10–20%) comes from ESI. This also implies that as concentrations of inhibitor and substrate increase above their K_{eq} and K_s values, relatively more product will be formed from ESI. Model C also implies that the complex has a K_s (βK_s,

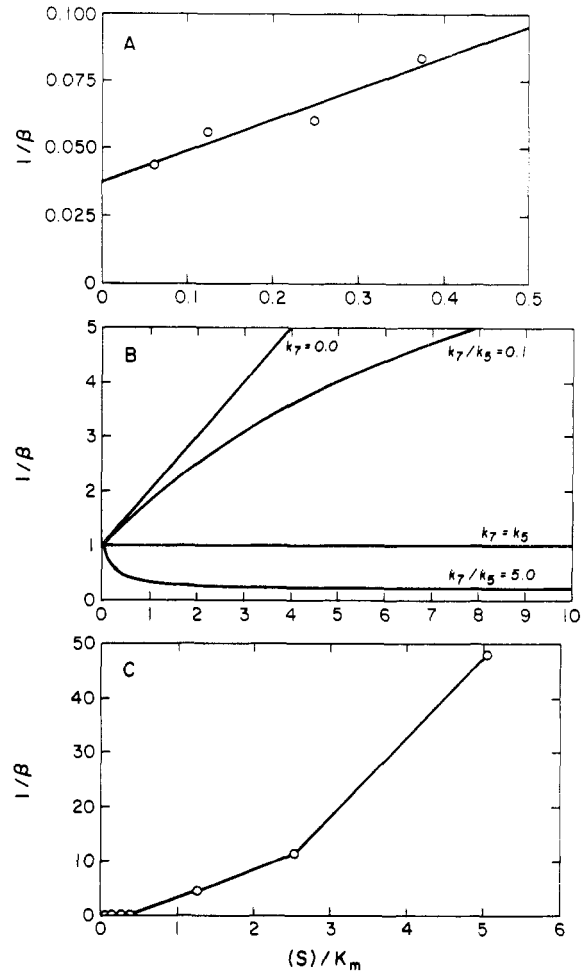

FIGURE 7: Rate of product formation curves plotted by the procedure of Cha (1976). (A) The substrate concentrations were less than K_m. The data are plotted as $1/\beta$ (from eq 2) vs. $[S]/K_m$. *p*-Nitrophenyl α-D-maltoside concentrations were from 1 to 6 mM. α-Amylase inhibitor concentrations were from 1×10^{-7} to 3×10^{-6} M. The α-amylase concentration was 5×10^{-7} M. The reactions were performed at 30 °C in standard buffer, pH 6.9. (B) Theoretical plots of $1/\beta$ (from eq 2) vs. $[S]/K_m$. These plots show what effects the relative values of k_7 and k_5 (model A) have on the curves. When $k_7 = 0.0$, the inhibitor is competitive with substrate. (C) The substrate concentrations were greater than K_m. The data are plotted as $1/\beta$ (from eq 2) vs. $[S]/K_m$. *p*-Nitrophenyl α-D-maltoside concentrations were 20–80 mM. α-Amylase inhibitor concentrations were 2×10^{-7} to 1×10^{-4} M. The concentration of α-amylase was 5×10^{-7} M. The reactions were performed at 30 °C in standard buffer, pH 6.9.

Table II: Rate and Equilibrium Constants for Models B and C When $[S] > K_m$

rate or equilibrium constants	model B	model C
K_{eq} (M)	$(4.06 \pm 7.42) \times 10^{-6}$	$(3.09 \pm 0.24) \times 10^{-5}$
k_1 (min^{-1})[a]	1.81 ± 2.5	3.05
k_{-1} (min^{-1})[a]	0.0087 ± 0.018	0.0
k_2 (min^{-1})		0.0
k_{-2} (min^{-1})		0.134 ± 0.025
α		1.27 ± 0.28
β		3.35 ± 1.24
k_p (min^{-1})	5.45 ± 0.25	7.39 ± 0.19
k_p' (min^{-1})		11.16 ± 0.30
absolute percent deviation	21.5	6.39

[a] k_{-1} and k_1 refer to model C; these same rate constants are represented by k_{-2} and k_2 in model B.

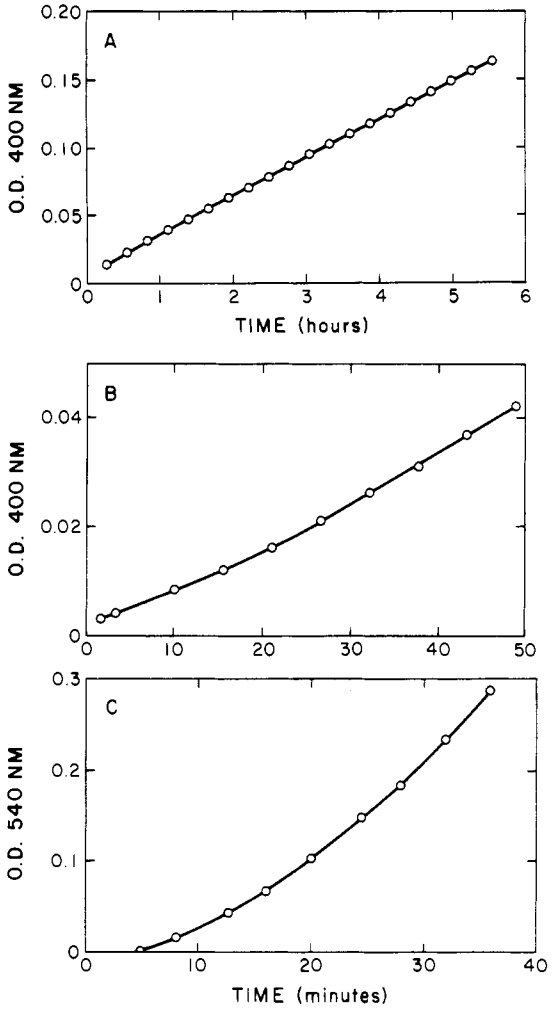

FIGURE 8: Rate of product formation in the presence of excess of inhibitor. (A) The reaction was started by the addition of α-amylase (5×10^{-7} M) to a mixture of 1×10^{-4} M α-amylase inhibitor (I to E = 200:1) and 20 mM *p*-nitrophenyl α-D-maltoside in standard buffer, pH 6.9, at 30 °C. (B) The reaction was started by the addition of *p*-nitrophenyl α-D-maltoside (20 mM final concentration) to a prior incubated mixture of 1×10^{-4} M α-amylase inhibitor and 5×10^{-7} M α-amylase (I to E = 200:1) at 30 °C in standard buffer, pH 6.9. (C) The reaction was started by the addition of maltrin M-100 (2.5% final concentration) to a previously incubated mixture of 5×10^{-6} M α-amylase inhibitor and 5×10^{-7} M α-amylase (I to E = 10:1), at 30 °C and pH 6.9 in standard buffer.

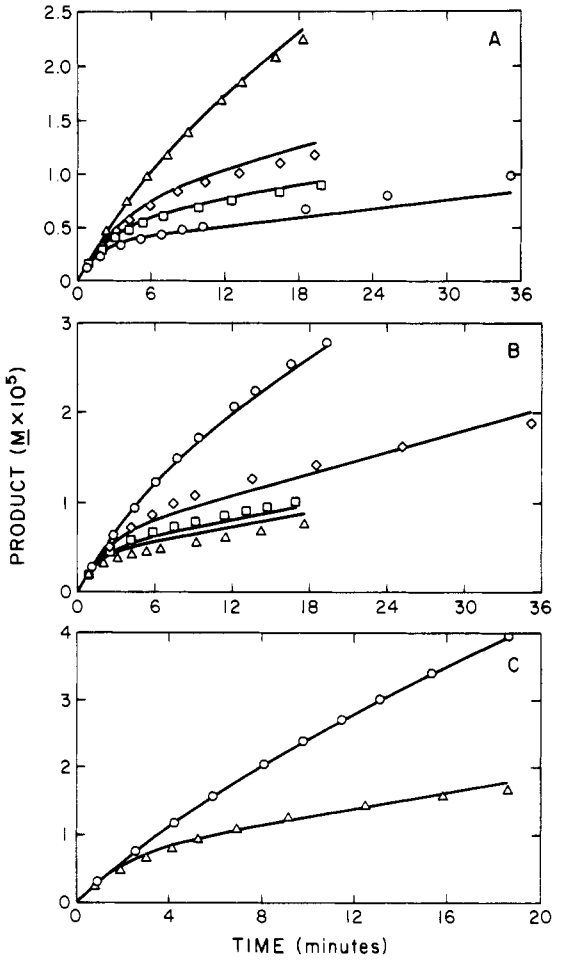

FIGURE 9: Rate of product formation curves fit to model C. Assays were performed at 30 °C in standard buffer, pH 6.9, with an α-amylase concentration of 5×10^{-7} M. Substrate concentrations were greater than K_m. (A) Substrate concentration was 20 mM *p*-nitrophenyl α-D-maltoside. α-Amylase inhibitor concentrations were 2.07×10^{-6} (△), 6.41×10^{-6} (◇), 1.12×10^{-5} (□), and 2.20×10^{-5} M (○). (B) Substrate concentration was 40 mM *p*-nitrophenyl α-D-maltoside. α-Amylase inhibitor concentrations were 5.22×10^{-6} (○), 2.17×10^{-5} (◇), 4.94×10^{-5} (□), and 7.03×10^{-5} M (△). (C) Substrate concentration was 80 mM *p*-nitrophenyl α-D-maltoside. α-Amylase inhibitor concentrations were 5.85×10^{-6} (○) and 1.06×10^{-4} M (△).

model C) value that is 3.4-fold greater than the α-amylase K_s value of 16.1 mM. These implications were shown to be correct by independent test methods.

In conclusion, the model that best fits the data (model C) requires two slow steps (EI → EI* and ESI* → ESI). It also requires that ESI be able to form product.

Discussion

The measured K_i for red kidney bean α-amylase inhibitor binding to porcine pancreatic α-amylase is 3×10^{-11} M (Powers & Whitaker, 1977b). This K_i is a combination of two steps as shown in the present work. The first step has a calculated K_{eq} of 3.09×10^{-5} M at pH 6.9. By stopped flow, two steps have been found in the binding of other enzymes to protein inhibitors. For example, the K_{eq} for the first step was 1.19×10^{-4} M for *Streptomyces* subtilisin inhibitor and subtilisin (Uehara et al., 1980), 2.3×10^{-5} M for soybean trypsin inhibitor and trypsin (Luthy et al., 1973), and 5×10^{-4} M for bovine trypsin inhibitor and chymotrypsin (Quast et al., 1974). Therefore, the initial K_{eq} for the interaction between red kidney bean α-amylase inhibitor and α-amylase is not much different from other protein–protein interactions.

The second (unimolecular, first-order; k_1 of model C) step of α-amylase inhibitor and α-amylase combination (EI → EI*) has a rate constant (k_1) of 3.05 min^{-1}. This same unimolecular reaction (first-order) step for other protein–protein interactions is 8400 min^{-1} for soybean trypsin inhibitor and trypsin, 21 000 min^{-1} for bovine pancreatic trypsin inhibitor and trypsin, and 46 400 min^{-1} for *Streptomyces* subtilisin inhibitor and subtilisin. This step for α-amylase inhibitor is very slow by comparison to the other three enzyme–inhibitor systems cited.

Red kidney bean inhibitor combines with α-amylase noncompetitively with substrate. The substrate, *p*-nitrophenyl α-D-maltoside, was used to perform the kinetic studies. The model that best fits all the data includes two slow steps. The forward (k_1, model C) step as mentioned above of 3.05 min^{-1} and a slower step (k_{-2}, model C) of 0.134 min^{-1}, which occurs after substrate combines with the complex of α-amylase amd α-amylase inhibitor (EI), permit the inhibitor to dissociate from α-amylase (in Table II, $k_1 = 3.05$ min^{-1}; $k_{-2} = 0.134$ min^{-1}; $k_{-1} = k_2 = 0.0$). The K_s' (βK_s, model C) for the complex was found to be 3.4-fold greater than the K_s for α-amylase and *p*-nitrophenyl α-D-maltoside of 16.1 mM.

The complex of α-amylase inhibitor and α-amylase gives

Table III: Error Analysis and Correlation Matrix of Rate and Equilibrium Constants for Model C

rate or equilibrium constants	Monte Carlo	support planes
	Error Analysis	
K_{eq} (M)	3.09 ± 0.23	0.24 −0.23
k_{-2} (min^{-1})	0.134 ± 0.015	0.028 −0.020
α	1.27 ± 0.25	0.32 −0.23
β	3.35 ± 0.93	1.41 −0.92
k_p (min^{-1})	7.39 ± 0.16	0.19 ND
k_p' (min^{-1})	11.16 ± 0.26	0.33 −0.24

Correlation Matrix

K_{eq}	α	β	k_p'	k_{-2}	k_p
1.0					
0.22	1.0				
0.62	−0.26	1.0			
0.30	0.98	−0.23	1.0		
0.48	−0.14	0.93	−0.16	1.0	
−0.88	−0.53	−0.40	−0.61	−0.35	1.0

the same spectral changes in the presence of maltose that are observed for maltose added to α-amylase (Powers & Whitaker, 1977b). The change in absorption associated with maltose binding to α-amylase indicates that maltose combines at the active site of α-amylase and causes a change in absorbance of an aromatic amino acid. The K_i for this change is the same as that determined kinetically (Elodi et al., 1972). Therefore, the active site of the α-amylase–inhibitor complex can still bind maltose.

Equilibrium dialysis experiments with ^{3}H-reduced acarbose indicated that the active site of α-amylase is not available to bind with acarbose when the enzyme is complexed with α-amylase inhibitor. This could mean that the active site of α-amylase is blocked on binding to the protein α-amylase inhibitor (not in agreement with the ability of maltose to bind). It could also mean that the active site of α-amylase in the complex is in a conformation that does not have the same affinity for acarbose. It could also mean that there is more steric hindrance in the enzyme–inhibitor that does not permit acarbose to bind, while the smaller maltose molecule can. α-Amylase combines with [^{3}H]acarbose with a one-to-one tight-binding stoichiometry, with some additional looser binding. The K_i of the tightly bound acarbose to procine pancreatic α-amylase is 9.7×10^{-6} M, which is in accordance with the kinetically determined K_i of 1.8×10^{-5} M for the same system (our laboratory).

The complex of red kidney bean α-amylase inhibitor and α-amylase binds to starch. This complex can be eluted with 0.5 M maltose, a competitive inhibitor of α-amylase. Buonocore et al. (1975) showed that gelatinized starch eluted α-amylase from a wheat amylase inhibitor–Sepharose affinity column. The data of Figure 8C indicate that the red kidney bean amylase inhibitor–α-amylase complex probably still has activity on maltin M-100. These data are indicative that the binding site of α-amylase in the complex is still accessible to starch. Final proof of this will require destruction of the starch storage binding site 30 Å removed from the active site of α-amylase (Payan et al., 1980) without loss of the starch-binding ability of the complex.

α-Amylase can be eluted from its complex with immobilized red kidney bean α-amylase inhibitor in the same manner that it is eluted from affinity columns of wheat α-amylase inhibitor (Buonocore et al., 1975). Maltose (0.5 M) at pH 6.9 causes a dissociation of the complex of α-amylase inhibitor and α-amylase.

From the above data, it appears that red kidney bean α-amylase inhibitor is not bound to the active site of α-amylase. This site is possibly still available in the enzyme–inhibitor complex to bind maltose. The substrate, *p*-nitrophenyl α-D-maltoside, can also bind to the complex and be converted to product. Larger substrates or inhibitors may also bind to α-amylase in the complex, but probably not with the same affinity that α-amylase alone has for them. When substrates or competitive inhibitors are present in high enough concentration, they allow α-amylase, by some slow process, to dissociate from the α-amylase inhibitor. The slow steps involved in getting the inhibitor on and off α-amylase are probably due to a conformational change in α-amylase (Powers & Whitaker, 1977b). This new conformation of the active site of α-amylase in the complex still has the same affinity for maltose as α-amylase alone but a changed affinity for acarbose and *p*-nitrophenyl α-D-maltoside. The changed affinity for acarbose and *p*-nitrophenyl α-D-maltoside shown by the complex in comparison with α-amylase could also be explained by steric effects of the α-amylase inhibitor being close to the active site of α-amylase.

Supplementary Material Available

Derivation of rate equations for model C (3 pages). Ordering information is given on any current masthead page.

Registry No. α-Amylase, 9000-90-2; acarbose, 56180-94-0; *p*-nitrophenyl α-D-maltoside, 17400-77-0; maltose, 69-79-4.

References

Banks, W., Greenwood, C. T., & Khan, K. M. (1971) *Carbohydr. Res. 19*, 252–254.

Bernfeld, P. (1955) *Methods Enzymol. 1*, 149–158.

Bieth, J. (1974) *Bayer-Symp. 5*, 463–469.

Buonocore, V., Poerio, E., Gramenzi, F., & Silano, V. (1975) *J. Chromatogr. 114*, 109–114.

Cha, S. (1976) *Biochem. Pharmacol. 25*, 2695–2702.

Cha, S. (1980) *Biochem. Pharmacol. 29*, 1779–1789.

Chandler, J. P., Hill, D. E., & Spivey, H. O. (1972) *Comput. Biomed. Res. 5*, 515–534.

Cuatrecasas, P., & Anfinsen, C. B. (1971) *Methods Enzymol. 22*, 345–378.

Elodi, P., Mora, S., & Krysteva, M. (1972) *Eur. J. Biochem. 24*, 577–582.

Green, N. M. (1953) *J. Biol. Chem. 205*, 535–551.

Gutfreund, H. (1972) in *Enzymes: Physical Principles*, p 205, Wiley-Interscience, New York.

Lowry, O. H., Rosebrough, N. J., Farr, A. L., & Randall, R. J. (1951) *J. Biol. Chem. 193*, 265–275.

Luthy, J. A., Praissman, M., Finkenstadt, W. R., & Laskowski, M., Jr. (1973) *J. Biol. Chem. 248*, 1760–1771.

Marchis-Mouren, G., & Pasero, L. (1967) *Biochim. Biophys. Acta 140*, 366–368.

Morehouse, A. L., Malzahn, R. C., & Day, J. T. (1972) U.S. Patent 3 663 369.

O'Connor, C. M., & McGeeney, K. F. (1981a) *Biochim. Biophys. Acta 658*, 387–396.

O'Connor, C. M., & McGeeney, K. F. (1981b) *Biochim. Biophys. Acta 658*, 397–405.

Payan, F., Haser, R., Pierrot, M., Frey, M., Astier, J. P., Abadie, B., Duee, E., & Buisson, G. (1980) *Acta Crystallogr., Sect. B B36*, 416–421.

Pick, K. H., & Wober, G. (1979) *Prep. Biochem. 9*, 293–302.
Powers, J. R., & Whitaker, J. R. (1977a) *J. Food Biochem. 1*, 217–238.
Powers, J. R., & Whitaker, J. R. (1977b) *J. Food Biochem. 1*, 239–260.
Quast, U., Engel, J., Heumann, H., Krause, G., & Steffen, E. (1974) *Biochemistry 13*, 2512–2520.
Schramm, M., & Loyter, A. (1966) *Methods Enzymol. 8*, 533–537.
Truscheit, E., Frommer, W., Junge, B., Muller, L., Schmidt, D. D., & Wingender, W. (1981) *Angew. Chem. 20*, 744–761.
Uehara, Y., Tonomura, B., & Hiromi, K. (1980) *Arch. Biochem. Biophys. 202*, 250–258.
Warner, T. G., & O'Brien, J. S. (1982) *J. Biol. Chem. 257*, 224–232.
Williams, J. W., & Morrison, J. F. (1979) *Methods Enzymol. 63*, 437–467.
Williams, J. W., Morrison, J. F., & Duggleby, R. G. (1979) *Biochemistry 18*, 2567–2574.

A Positional Isotope Exchange Study of the Argininosuccinate Lyase Reaction†

Frank M. Raushel* and Lisa J. Garrard

ABSTRACT: ^{15}N nuclear magnetic resonance spectroscopy was used to follow the positional isotope exchange reaction of bovine liver argininosuccinate lyase. The enzyme was shown to catalyze the N-3–N-2 positional nitrogen exchange in [3-^{15}N]argininosuccinate in the presence of excess arginase. The ratio of the positional isotope exchange rate and the rate for net substrate turnover is less than 0.15 at low levels of fumarate but increases to a limiting value of 1.8 at high fumarate. These data have been interpreted to mean that the dissociation of fumarate and arginine from the ternary enzyme complex is random although fumarate is released at least an order of magnitude faster than is arginine from this complex. The rate constant for the release of fumarate from enzyme–arginine–fumarate is at least 6 times faster than the turnover number of the reverse reaction of argininosuccinate lyase. The lower limit for the release of arginine from this same complex is 0.5.

The positional isotope exchange (PIX) technique was first developed by Midelfort & Rose (1976) to investigate the kinetic competence of γ-glutamyl phosphate as a reactive intermediate in the glutamine synthetase reaction. More recently, this technique has also been applied to the reactions catalyzed by carbamyl-phosphate synthetase (Wimmer et al., 1979; Raushel & Villafranca, 1980), farnesylpyrophosphate synthetase (Mash et al., 1981), pyruvate kinase (Lowe & Sproat, 1978), and others. Thus far, this method has been primarily used to determine whether these enzyme-catalyzed reactions proceeded via stepwise or concerted reaction pathways. For example, in the carbamyl-phosphate synthetase reaction the kinetic competence of both carboxy phosphate (Wimmer et al., 1979; Raushel & Villafranca, 1980) and carbamate (Raushel & Villafranca, 1980) was demonstrated via positional isotope exchange with [*β,γ-bridge*-^{18}O]ATP and carbamyl [*bridge*-^{18}O]phosphate, respectively.

The positional isotope exchange technique can also be used to conveniently measure the partitioning of enzyme-bound intermediates and complexes and to measure individual rate constants or ratios of rate constants in these mechanisms. These results can then be combined with other techniques such as stopped-flow or rapid-quench experiments to obtain individual rate constants and information on the rate-limiting steps. In the carbamyl-phosphate synthetase reaction, the positional isotope exchange data were used to establish that the formation of the intermediate carboxy phosphate was probably rate limiting for the overall chemical reaction.

Scheme I

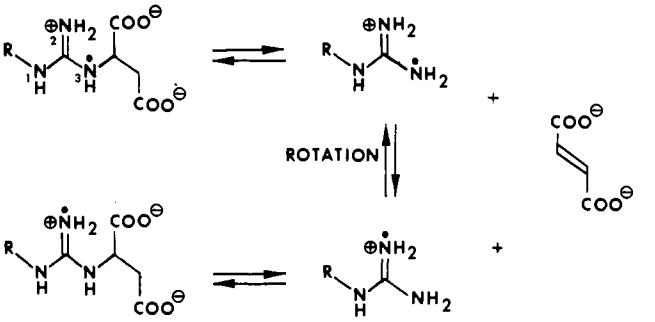

All of the PIX reactions examined to date have followed the isotopic exchange of ^{18}O and ^{16}O atoms in phosphoryl or carboxylate groups. A previously unrecognized group in which a positional isotope exchange reaction can occur is the guanidino group of arginine and creatine. Shown in Scheme I is an outline for the detection of positional isotope exchange in the argininosuccinate lyase reaction. When argininosuccinate that is labeled with ^{15}N at N-3 is cleaved by argininosuccinate lyase to enzyme-bound arginine and fumarate, the two guanidino amino groups are able to equilibrate via rotation about the carbon–nitrogen bond. Resynthesis of argininosuccinate will form, with a 50% probability, argininosuccinate labeled with ^{15}N at the N-2 position. To ensure that this exchange reaction is occurring only via enzyme-bound ligands, arginase can be added to the reaction mixture to keep the free arginine concentration at zero.

In this paper, we have applied the positional isotope exchange technique to the argininosuccinate lyase reaction. By measuring the positional isotope exchange rate relative to the net chemical turnover of argininosuccinate as a function of

† From the Department of Chemistry, Texas A&M University, College Station, Texas 77843. *Received September 28, 1983.* This research has been supported by the National Institutes of Health (AM-30343) and the Robert A. Welch Foundation (A-840).

0006-2960/84/0423-1791$01.50/0